TACTICAL WEAPON
GACIAC
GUIDANCE & CONTROL
INFORMATION ANALYSIS CENTER

GACIAC PR 92-01

PROCEEDINGS OF THE SECOND AUTOMATIC TARGET RECOGNIZER SYSTEMS AND TECHNOLOGY CONFERENCE

Volume II - Unclassified

17-18 March 1992

Conducted at:

Center for Night Vision and Electro-Optics
Ft. Belvoir, Virginia

Sponsored by:

Defense Advanced Research Projects Agency (DARPA)
DoD Working Group on Automatic Target Recognition (DoD WGATR)
Automatic Target Recognizer Working Group (ATRWG)
Joint Services Guidance and Control Committee (JSGCC)

Published by GACIAC
IIT Research Institute
10 West 35th Street
Chicago, Illinois 60616-3799

SCALE-SPACE POLYGONALIZATION OF TARGET SILHOUETTES AND APPLICATIONS TO MODEL-BASED ATR[1]

13 February 1992

David C. MacEnany and John S. Baras[2]
AIMS, Inc.
6159 Executive Blvd.
Rockville, MD 20852

ABSTRACT

Economic descriptions of shapes and objects are essential for model based ATR. In addition to object silhouettes, geometric features such as corners and simplified representations such as polygonal approximations can be used to reduce shape description complexity. Here we analyze the polygonal approximation of object silhouette boundaries. Robust polygonalization for ATR requires the construction of polygonal approximations in various scales; namely polygons preserving features of the boundary with varying resolution. In this paper we introduce the notion of scale-space polygonalization. Scale-space polygonalization allows for the generation of polygonal approximations across a range of resolutions and achieve vertex localization which is uniform in scale. The notion of *scale* or *resolution* for a polygon involves the distances between its vertices and the magnitude of its vertex angles. Fine scale implies high resolution of the details of boundary contours while coarse scale implies only gross details of boundary contours with a consequent reduction of both computational and descriptive complexity. The polygonalization methods and algorithms presented here are novel in that we control the reduction of the contour complexity by adjusting resolution parameters which have a natural interpretation and achieve vertex localization which is *uniform in scale* and *persistent in scale*. These polygonalized boundaries can be used to generate a *target fingerprint* across a range of scales. Scale-space polygons are important for ATR because they provide a way to reduce the complexity of digitized planar curves consisting of polygons having hundreds of sides to polygons of about a dozen sides, while still capturing the essential features of the model silhouette. This is desirable because shorter polygonal descriptions yield faster correlations and matchings and reduce the overall computational complexity of the ATR problem. We show how scale-space polygonalization can be used to obtain efficient representations of targets, and fast matching algorithms. We also show how scale-space polygons can be used to obtain stable edges from noisy images. We demonstrate these results on examples involving synthetic FLIR data and CAD target models.

1.0 INTRODUCTION

An essential ingredient to model-based automatic target recognition (ATR) is a model construction methodology. Such a methodology, in order to be successful, must respect the tight coupling which exists between model representation and model recognition. For maximum flexibility, it should also permit the construction of models based on real-world (field) imagery as well as simulated (synthetic) imagery with equal ease. In addition, the methodology should construct a catalogue of models with controlled model complexity, *i.e.*, economic models with a systematic organization.

In this paper we consider some low-level representation issues of our target model construction methodology which employs object models consisting of combinations of boundary representations in the form of polygonal contours.

[1] Work partially supported by contract No. DAAB07-90-C-F425 from U.S. Army CECOM, through the C²NVEO. COTR: Ms. T. Kipp C²NVEO.

[2] This author is also affiliated with the Electrical Engineering Department and the Systems Research Center, University of Maryland, College Park, MD 20742

The discussion will focus on one of the methods we use to extract multiresolution polygonal contours from digitized curves, representing object silhouettes, obtained from both CAD models and field imagery using various sensors.

Digital planar curves in the form of noisy "pixel chains" are the starting point for our multiresolution polygonalization algorithms. By a pixel chain we mean a sequence of integer couples. Proper filtering of raw digital curve data yield *polygonal contours* which admit model representations from CAD descriptions of physical target models or actual image data. CAD descriptions lead to raw digital curves in a straightforward manner, be they geometric descriptions as obtained through the use of a solid modeling package such as BRL-CAD and intended for use with camera sensors, or geometric descriptions extended via thermal modeling and simulation, as is made possible through the use of thermal modeling packages such as PRISM or BISP, or analogous CAD model extensions for use with LADAR. As an alternative to CAD descriptions, one may construct, or be forced to construct, model representations directly from "field imagery" using segmentation methods. Image segmentation methods implicitly model a real-world scene as a collection of 3-dimensional objects which by viewpoint projection generate a planar arrangement of homogeneous regions corresponding to homogeneous surface potentials in the image of the original scene. The goal of image segmentation is to take a real-world scene that has been sampled down to a rectangular grid by some input sensor and corrupted by diverse noise sources involved in the total image formation process, and then compute an estimate of the projected planar arrangement of homogeneous regions. This is usually done as a first step in inferring the original 3-dimensional scene, but in our case it is a first step in extracting a polygonal model induced by the segmentation boundaries of the regions. A key feature of the segmentation model is that the definition of homogeneity is a design construct which may, for instance, refer to luminance, chrominance, texture, *etc.*, in the case of vision data, or absolute range, relative range, *etc.*, in the case of LADAR and millimeter wave data, or absolute and relative temperature in the case of FLIR or some multi-sensor combination of these.

As an example, one may model the visible image of a 3-dimensional object, whether it be a ray-traced CAD image or one obtained from field imagery, by a quantized space of 2-dimensional bounding surfaces, and from a fixed viewpoint, each 2-dimensional surface may in turn be modeled using a 1-dimensional polygonal approximation to its (closed) silhouette contour. Such a silhouette representation is a starting point primitive upon which to build more complex models. For instance, edge boundaries internal to the surface circumscribed by the silhouette may also be modeled using polygonal approximations to their (not necessarily closed) contours.

In Figure 1 we show a composite silhouette built up from a polygonalized silhouette and the analogously polygonalized internal boundaries (quantized to an underlying image grid, not shown). The internal boundaries model regions of similar temperature (thermal homogeneity). This shows how polygonal silhouette models can be augmented with additional internal boundaries based on the *a priori* knowledge of the thermal inhomogeneity characteristics of the target. In Figure 2 we show these two polygonal models overlaid on (synthetic) FLIR images, one of a target which is uniformly "hot," and therefore only requires silhouette information for high confidence recognition and one of a target which has a non-uniform temperature distribution, hot and cold spots in predictable areas.

The union of such internal boundaries and silhouettes yields a hierarchy of geometrical models for the given object extended by *a priori* knowledge regarding such quantities as expected luminance or relative contrasts of the various planar regions segmented by the polygonal contours. Of course, this approach is equally applicable to infrared sensor data, LADAR data, *etc.*, in which the segmentation topology can instead be augmented with expected temperatures or temperature gradients or relative range differences, *etc.*, for the different regions of homogeneity.

These concerns have lead us to investigate hierarchical model representations built up from polygonal approximations to planar curves.[3] In this paper, we will address multi-resolution polygonal approximations of digitized planar curves and mainly limit the discussion to closed contours as derived from silhouette boundaries. Multi-resolution polygonal approximations lead to compact descriptions which decrease on-line memory requirements and can facilitate effective tree-structured recognition. The notion of a multi-resolution polygonal approximation derives from the fact that a single polygonal approximation to a target silhouette is neither desirable nor warranted. For example, we routinely extract digitized silhouette contours from both field imagery and BRL-CAD ray-tracings in which the digitized silhouette contours of military targets are essentially polygons having hundreds of vertices. However, the same target silhouette at 1km and 4km, although it is similar in "shape," does not possess the same polygonal complexity. Obviously, this is due to the difference in resolution at the two ranges. The method we present permits

[3]Note that the collection of planar curves includes all waveforms, so much of what we say here can be interpreted in this more restricted context. This has important implications regarding model-based multi-sensor fusion.

one to model resolution as a function of range.

An innovative and significant component of our method is the systematic construction of polygonal silhouette approximations at different resolutions (scales). Thus, we obtain multiresolution representations of silhouettes. There are other techniques which can produce multiresolution representations of one and two dimensional data, *e.g.*, wavelets. However, our methods have two unique qualities associated with them, in that they localize significant features of the silhouette, such as maximal curvature points, at the same arc location at all resolutions, and features which are present at coarse resolution are also present at fine resolution. Other methods based on convolution by a rapid-decay kernel followed by thresholding, or even wavelets, do not share these important properties. We achieve this essentially because our methods are nonlinear. *Uniform localization* of features is essential for recognition, because it preserves the characteristic shape of the silhouette at all resolutions. *Persistent localization* is key since it permits a systematic, *hierarchical* organization of models indexed by resolution.

Polygonal approximations to target silhouettes are important for two reasons: (*i*) They reduce substantially the memory required to store many views of the silhouettes of many targets; (*ii*) They lead to target matching and target silhouette retrieval algorithms that are faster by orders of magnitude.

The computational and memory requirements associated with target silhouettes are explosive, due to the variation of the viewing angle (i.e., the direction in 3-D space from which we view the target) and range. Substantial reduction of the resulting complexity is essential. Our methods address systematically the economy (complexity of the target model) in two fundamental ways. The first has to do with the viewpoint variation of the target silhouette. It is not difficult to establish using experiments with CAD or field images of targets that, depending on the range, the silhouette does not vary significantly for every 1° variation in the viewpoint. In simpler terms, we do not store the target silhouette for every 1° of aspect variation. We have developed systematic methods to extract *exactly* those equivalence classes of target silhouettes (with respect to viewpoint variation) which must be stored in order to guarantee a given recognition performance. We have approached this problem in an innovative way as a signal quantization problem and have used sophisticated versions of Vector Quantization (VQ) in the resulting algorithms. The resulting algorithms are the first to incorporate such methods into this problem. These computations, done at different scales (ranges) lead to the construction of the aspect graph [62] of a target, which represents an efficient, hierarchical and progressively finer representation of target models based on silhouettes. The second addresses in a similar fashion the variation of the silhouette with respect to range. Variations in range can be mapped into variations in resolution by our methods. Via a scale-space diagram we can easily identify the finite set of polygons needed to be stored to capture the entire variation of the silhouette with respect to range. These constructs address effectively and in a hierarchical manner the introduction of new vertices as the resolution becomes finer.

Our methods address also the ranking (or saliency) of the silhouette features. Polygonal approximations of the silhouette lead to the identification of important features such as convexities, concavities, long straight lines and sharp corners of the silhouette, characterized and ranked by the local (discrete) curvature. In a way, these polygons, viewed as piecewise constant curves in tangent-angle *vs.* arc-length space, provide *bar-code* representations of the target silhouette across resolution. From the bar-code, the silhouette can be progressively recaptured with increasing fidelity by generating higher order polygons. In addition, the polygons simplify the identification of features, or groups of features, by considering them as parts of piecewise constant curves. This observation can be exploited in matching algorithms by utilizing more local features rather than more views of the target silhouette, which as mentioned above are redundant.

The problem of polygonal approximation of digital planar curves has received considerable attention in the literature [1]–[58]. This remains true with more recent investigations increasingly emphasizing the notion of resolution. In part this attention is due to the fact that such representations are often a first step in shape analysis and classification. Most past approaches [1]–[55] to the basic problem can be understood as the solution to one of two problems which are the dual of one another: *digital curvature filtering* and *piecewise line fitting*. In the first approach the goal is to locate a set of "dominant points" by filtering the pixel chain with various angle and corner detection schemes and achieve polygonalization by "connecting the dots" as defined by the dominant points considered as vertices. Schemes based on digital curvature filtering, or *corner detection*, necessarily entail some *ad hoc* definition of "digital curvature," since strictly speaking curvature is everywhere well-defined only for smooth planar curves. The most frequently cited psychophysical motivation for this approach is Attneaves' cat [60], the well-known dominant point polygonalization of a line-figure of a cat which people instantly recognize as a feline at a

glance. The polygonalization approach dual to curvature filtering is to directly fit line segments by various piecewise linear filtering algorithms, and then locate the vertices at the intersections of the consecutive line segments so found.[4] The approach we describe here combines corner detection and line fitting in one algorithm.

Various algorithms in the corner detection category are discussed in [1]–[12]; algorithms in the segment detection category are considered in [13]–[55]. The most widely used segment fitting algorithms are reviewed in [38], [32], [48], [51] and compared in [51] 55]; the similarly popular corner detection algorithms are surveyed and compared in [12]. Algorithms which combine elements of both are considered in [56], [58]. The method closest to our own, and in fact motivated the approach, is described in [58], although our method differs in key aspects and enjoys persistence in resolution. Another approach to multiresolution shape analysis is given in [59] which is based on the geometric heat equation. This approach leads to qualitative descriptions of shape across resolution, but so far has not lead to shape compression and organization.

2.0 SCALE-SPACE POLYGONALIZATION

We now focus the discussion on an efficient algorithm for multiresolution polygonalization of digitized silhouette contours. The version of the algorithm given here requires $n = 5$ input parameters, although there are versions of the basic algorithm which require $n = 0, 1, 2, 3, 4$, or all five parameters depending on the modeling situation. These parameters are refered to as resolution parameters since they closely couple notions of spatial detail and sensor noise. For a fixed n-tuple of resolution parameters, we call the reduced complexity polygonal approximation of a digitized boundary contour a *characteristic polygon* for that n-tuple. Characteristic polygons are important for the following reasons. First, they provide a way to reduce the complexity of digitized silhouettes consisting of polygons having "too many" irrelevant sides due to noise and grid quantization. This of course is desirable since shorter silhouette vectors yield more robust correlations and more compact storage of reference patterns. Second, a characteristic polygon greatly simplifies a model boundary but still captures the essential features of the model silhouette, namely points of critical curvature: the location of corners, and long, straight lines. Third, our methods let us control the reduction in the complexity of the boundary description as a function of range (spatial scale) and noise by means of adjusting the resolution parameters. The interpretation of the resolution parameters in this context is a natural one: scale parameters control the deviation of the boundary contour from long straight lines between the vertices of the polygon while *angular* sensitivity parameters control the size of the angles between the two edges of each vertex of the polygon. Fourth, characteristic polygons are a tool to obtain stable edges from noisy images in an efficient manner. We can compute characteristic polygons very quickly using standard hardware and software. Finally, the *scale-space uniformity* property of weak continuity methods [65] in the context of polygonalization yields the remarkable uniformity property of the vertices as a function of resolution: Vertices which exist at coarse scale exist also at fine scale *and occupy the same positions* along the arc of the target silhouette. Scale-space uniformity gives access to polygonal edges and vertices that can be counted on and a multiresolution hierarchy of polygons that can be counted down, as will be shown.

Consider a digitized contour $\vec{d}$ of N pixel chain locations, an ordered sequence of data pairs (x_i, y_i) with $\vec{d}_i = [x_i\ y_i]^T$, $i = 1, \ldots, N$. Our procedure has two main parts, each involving the minimization of a variationally defined energy functional [65], [72]. In the first main part, we weakly smooth $\vec{d}$ to obtain $\vec{f}$. From $\vec{f}$ we obtain the subsampled chain $\vec{g}$ which is a polygonal contour ready to have its tangents read off. This yields the turning function θ of $\vec{g}$ which gives the angles of the sides of $\vec{g}$ as a function of the arc-length of the silhouette measured from some reference vertex. Next, in the second main step, we minimize another non-convex energy functional involving θ. The last step is to locate and connect the critical points of $\vec{g}$ according to the discontinuities in θ. We give a breakdown of the main steps as follows.

Polygonalization Procedure.

STEP 1: *Weak Smoothing of the Digital Contour.*

The purpose of this step is to *weakly* low-pass filter the digital contour in order to compute a faithful digital tangent even in the presence of very noisy data. This pre-conditioning is necessary to extract the so-called *turning function* discussed below. Computation of the turning function involves a one-time trigonometric calculation for

[4] More generally, one may go to higher order schemes. For instance, in [53] a switched first and second order scheme is used in an attempt to decompose a digitized contour into a sequence of linear and circular segments. Our method extends to higher orders in a natural way.

angles at successive vertices. Alternatively, one could design the entire polygonalization process as a variational problem defined directly on the chain data with an in place estimation and penalty calculated according to a full, nonlinear characterization of the approximate digital curvature, but this is computationally very expensive and we found it to offer little over the proposed approach. The approach taken here uses a rotationally invariant, quadratic approximation to the "curvature" as a one-time pre-conditioning step followed by a one-time angle extraction step.

The prerequisite to Step 3 below is cleaning up the noise in the tangents of $\vec{d}$. Since we desire a tangent which is not too noisy it is necessary to smooth the boundary data. However, since we also desire a tangent which respects corners—discontinuities in curvature—we only wish to smooth the boundary in a piece-wise fashion. Hence, we employ methods based on ideas of weak-continuity [65]. We define the digital energy functional,

$$\mathcal{E}(\vec{f}) = \sum_{i=1}^{N} ||\vec{d}_i - \vec{f}_i||^2 + \lambda^2 ||\vec{f}_i - \vec{f}_{i-1}||^2 (1 - \ell_i^1) + \mu^4 ||\vec{f}_{i+1} - 2\vec{f}_i + \vec{f}_{i-1}||^2 (1 - \ell_i^2) + Q, \tag{1}$$

where $\vec{f} = \{\vec{f}_i\}_{i=1}^N$ is the 'fit' to the digital contour, Q consists of a penalty of α for each discontinuity in $||\vec{f}_i - \vec{f}_{i-1}||$ and a penalty of β for each discontinuity in $||\vec{f}_{i+1} - 2\vec{f}_i + \vec{f}_{i-1}||$ and the ℓ_i^1, ℓ_i^2 denote binary indicator variables which flag the presence of first and second order discontinuities. The first term in the sum is understood to model "faithfulness to the data," in the sense that a minimizer of the energy functional must keep this term small relative to the other terms. This zero-order term provides the only connection between the fit and the data; the remaining terms are entirely internal first and second order penalties on the fit. The second term levies a cost on the local length contributions of each segment; this term can be used to detect breaks in contours. The third term penalizes local deviations from straight-line behavior in the resulting fit by penalizing non-zero curvature in the sense of weak continuity. By itself, this term is a poor approximation to the local curvature but its redeeming quality is its rotational invariance and quadratic form and the fact that it results in good performance on a global level. A by product of its definition is that it also encourages shorter solutions and we exploit this "bunching" property below to derive a "cardinality filter." If the contour is closed, the fit is considered to "wrap-around" at the endpoints, otherwise one must handle the endpoint conditions appropriately. The Q term, through the action of the ℓ^1 and ℓ^2 indicator vectors, "cuts off" either one or both of the first and second order penalties if it is "cheaper" to declare a zero- or first-order discontinuity at a given chain point and incur a maximum cost of α and/or β. If there were no penalties for the discontinuity terms then the optimal solution is simply the solution to a pentadiagonal linear system. However, it is essential to include the discontinuity penalties and this results in a non-convex energy functional which cannot be minimized by usual gradient descent. However, it can be minimized using the Graduated Non-Convexity (GNC) algorithm [65] and GNC-like algorithms [64], [69]. If real-time operation is required, the minimization can be performed by recasting it in a neural net framework in which the indicator variables are the outputs of a sigmoidal nonlinearity [74], [75]. Three "before and after" examples of this step of the algorithm run on target silhouette data are given in Figure 3. The piecewise low-pass filtering property of the weakly smoothed chain is clearly evident.

STEP 2: *Chain Subsampling.*

A principal effect of the linear length penalty term and a by product of the quadratic curvature smoothing term is to encourage "bunching" of the chain points, especially when the chain has been extracted using a simple 4-way contour follower [25]. Removing this redundancy is advantageous and straightforward. Let $\vec{f}$ denote the fit obtained by minimizing $\mathcal{E}$; note that the components of $\vec{f}$ are no longer necessarily integer valued. Begin by quantizing $\vec{f}$ to an integer valued chain denoted $\vec{\mathrm{f}}$. Then, proceed sequentially along $\vec{\mathrm{f}}$ deleting points from $\vec{f}$ if successive points of $\vec{\mathrm{f}}$ quantize to the same location. Call the resulting subsampled chain $\vec{g}$.

STEP 3: *Calculation of the Turning Function.*

The right continuous turning function $\theta(s)$ of $\vec{g}$ can be defined as follows. If starting from the first chain point, $\vec{g}_1$, we let s denote some distance around the perimeter of $\vec{g}$, then $\theta(s)$ denotes the angle made by the initial segment $\vec{g}_1\vec{g}_2$ and the polygonal segment of $\vec{g}$ at that distance; if s is the distance to some vertex, $\theta(s)$ is the angle made by $\vec{g}_1\vec{g}_2$ and the next segment at $s+$. For example, consider the initial segment, $\vec{g}_1\vec{g}_2$, of $\vec{g}$ as providing a zero reference angle so that θ is zero on $\vec{g}_1\vec{g}_2$. At $s = ||\vec{g}_2 - \vec{g}_1||$ the turning function $\theta(s)$ has a discontinuity of size given by the angle that the directed segment $\vec{g}_2\vec{g}_3$ makes with the directed segment $\vec{g}_1\vec{g}_2$ so that $\theta(s-) = 0$ while $\theta(s) = \theta(s+) = \angle(\vec{g}_1\vec{g}_2, \vec{g}_2\vec{g}_3)$. The rest of $\theta(s)$ is defined analogously so that the distances between successive discontinuities encode the lengths of the sides of the digital polygon, while the jump sizes $\theta(s+) - \theta(s-)$ encode the change in vertex angle. If one

is not working with polygons, then it may be necessary to also keep track of the so-called winding number [58], i.e., the number of complete 2π cycles. The top two graphs of Figure 4 show two turning functions extracted with and without pre-conditioning via weak smoothing of the pixel chain for the raw digital curve of the M113 APC in Figure 3. The necessity of the pre-processing by the weakly smoothed chain is clearly evident in the graph of the turning function.

STEP 4: *Weak-String Algorithm Applied to the Turning Function.*

The idea of performing an analysis on the $\theta(s)$ curve to extract critical points of curvature is not new. Its utility was convincingly argued in [57]. However, previous approaches to this analysis were based on scale-space filtering [76] with Gaussian kernels. These approaches were plagued by the lack of uniformity of discontinuity locations in Gaussian scale-space. As a result, the promise of the *curvature primal sketch* [57] remained unfulfilled. These developments were soon followed by the contributions in [58] who realized that their weak continuity methods enjoy uniformity in scale, and considered the application of their nonlinear *weak string* filter technique to turning functions. Applying their results is a crucial step in the task of obtaining a characteristic polygon, however, we emphasize that without the preprocessing via weak smoothing, their approach used directly gives results which we have found to be quite difficult to interpret automatically under the severe noise conditions present in noncooperative, military target recognition. Hence, after the pre-conditioning step, we use the variational approach once again and minimize the weak string energy functional [65] for the turning function,

$$\mathcal{E}_\theta(\phi) = \int |\phi(s) - \theta(s)|^2 + \lambda^2 \int |\phi'(s)|^2 + \alpha P, \tag{2}$$

where the λ and α in the definition of $\mathcal{E}_\theta$ are not necessarily the same λ and α as in $\mathcal{E}$ above. In the context of this minimization the two parameters α and λ interact in a natural manner with direct implications for the segmentation of planar contours. Following [58] these are:

λ—*Natural Scale Parameter:* Contour details which are smaller than λ get smoothed out and contour features which are separated by more than λ units are treated almost entirely independently in the smoothing process;

α—*Resistance To Noise:* If α is larger than twice the noise variance then 'false' discontinuities will not occur;

Φ_0—*Angular Sensitivity:* Large isolated changes in the angles between successive polygonal segments—angular discontinuities—will be detected if and only if their angle exceeds $\Phi_0 := \sqrt{2\alpha/\lambda}$;

We emphasize that this energy functional can be minimized using the GNC algorithm [65] as discussed here, or other continuation methods such as [69], [64], and that no linear filter with thresholding, so-called non-maxima suppression, enjoys such localization accuracy [65], [72] in the presence of noise. An application of the weak string to a turning function is given in the bottom graph of Figure 4.

STEP 5: *Edge Extraction.*

As is usual with weak continuity methods, the edges are quite simply extracted by a simple thresholding step, namely, we mark an edge at s if, $|\phi'(s)| \geq \sqrt{\alpha}/\lambda$.

STEP 6:—*Back-Indexing.*

Edges marked on the fit to the $\theta(s)$ curve are back-indexed into the contour $\vec{g}$. Note that the edges in $\theta(s)$ correspond to corners along the weakly smoothed chain. Connecting the corners so obtained results in what we call the *characteristic polygon.* We note that as the scale and angular sensitivity parameters increase, vertices will drop out of the characteristic polygon, however, *no additional vertices will appear* as we ascend scale/sensitivity space. This is the scale-space uniformity enjoyed by characteristic polygons: A vertex, or corner, at a coarse resolution persists at all finer resolutions and *occupies the same location.*

An important point to address is the selection of resolution parameters. Some of the alternative methods available are: to remove them via optimization according to some criterion such as *cross-validation* [67]; to adjust them adaptively to the local character of the given curve using appropriately adaptive versions of GNC algorithms [65]; to employ an extension of Witkin's stability notions of scale-space filtering [76] in an attempt to extract composite descriptions which emphasize features at different scales simultaneously; or to simply store the entire scale-space description, or some quantized description, using the compact hierarchical storage afforded by the uniformity property

and *index into* such a description by resolution as appropriate. On the other hand, with proper modeling only a small number of "slices" of scale-space, i.e., only a small number of polygonalizations at selectively quantized n-tuples of the resolution parameters, are required for most problems in the ATR context.

3.0 UNIFORM AND PERSISTENT LOCALIZATION IN SCALE-SPACE

One immediate consequence is that the multiresolution description of a polygon, as described in section 2, has a very compact representation. In the context of computational geometry such a representation for a convex polygon is called a *balanced hierarchical representation* [70] which leads to advantageous computational properties.

Using characteristic polygons computed at different scales we can construct the graph shown in Figure 5 (top). Here the abscissa indicates the arc-length along the target silhouette perimeter from a reference point, while the ordinate indicates the resolution. We see that, as expected, we get a representation where features (critical curvature points) generate vertical lines as we move across scale. This should be contrasted with the algorithms of Witkin [76], which suffer from the nonuniformity of methods based on convolution with rapidly-decaying kernels followed by thresholding. This is the diagram we call the scale-space diagram, or scale-space filtering in the sense of Witkin. In this terminology Figure 5 illustrates the scale-space diagram of an M113 APC.

The scale-space diagram just constructed has many utilities in discovering organization in the target silhouette and in ATR strategy development. In addition it is useful in understanding feature stability with respect to resolution (which is strongly influenced by range). A notion of feature stability was proposed by Marr, who without detailed justification, proposed the "coincidence assumption," that only features which spatially coincide at all scales are physically significant. He further described the image by the zero-crossings in its convolution with the laplacian of a gaussian, at several fixed scales. Experience and experiments have shown subsequently that the latter assumption fails in that variable scales need to be incorporated.

One can think of the scale-space diagram (illustrated in Figure 5 for an M113 APC) as some sort of fingerprint of the target. Indeed as Witkin [76] observed, one of the fundamental values of scale-space descriptions, is the discovery of organization and structure in a signal by relating the singular points (points of extreme curvature) across scale. Since he used non-maxima suppression via convolution and thresholding, his scale-space representations did not provide uniform localization of features. Our algorithm provides uniform and persistent localization of features across scale as shown in the bottom of Figure 5.

Refering to Figure 5, the vertical lines represent a set of distinguished points, namely the vertices of the polygonal approximation to the silhouette. The height of each line corresponds to the resolution, which by transformation incorporates both the significance of the corresponding feature via the size of the vertex angle and the scale (range). Thus, if we draw a line parallel to the horizontal axis at some coordinate σ_*, and note the points of intersection with the vertical lines of the scale-space diagram, we obtain a polygonal approximation at that resolution. We immediately see that in order to store all the variations of the silhouette with respect to resolution we only need to store the polygons corresponding to those values of σ_* at which, as we traverse the diagram downwards, new vertices appear. The corresponding catalogue of polygons provides a hierarchical, localized data structure which can efficiently guide an ATR associated search for identifying a target beginning from a coarse polygon and progressively adding vertices as needed for identification and discrimination. Further reduction in storage results by considering only *stable polygons*, i.e., polygons that do not change quickly with small changes in the resolution parameter σ_*. Indeed, in practice it will be impossible to detect such small and "rapid" variations of the local character of the target silhouette, so it is not necessary to store all these polygons. As a result of these two notions a fairly reduced target model results, in that only a small number of polygons is needed in order to capture the silhouette variation with respect to range. An of course, the hierarchy is nested for compact storage.

An additional application of the scale-space diagram is that in the case of obscured targets, we can use a portion of the silhouette arcs that are present, to organize the search for the target recognition based on the local features and their relationship across scale as indicated by the corresponding portions of the scale-space diagram. It is in this sense that the scale-space diagram provides a "fingerprint" for a target.

Finally, we have developed a notion of feature stability which is an extension of that of Witkin [76]. The basic idea stems from the fact that as we traverse the scale-space diagram from coarse resolution to finer resolution, the appearance of a new vertex can be translated to a notion of stability of the line segment connecting the two vertices lying above the new one. Depending on the relationship of certain geometric parameters we can quantify the stability of a feature, and that of a polygonalization along these lines of reasoning. These results will be described elsewhere

in detail.

4.0 COMPUTATIONAL RESULTS

4.1 RESULTS FOR BRL-CAD DATA

The results of our polygonalization procedure are shown in Figure 6 through Figure 8 for each of three targets of interest at 10° from head on, namely the M60 tank, the M113 armored personnel carrier and the M35 truck. In the first column of Figure 3 we show the respective digital silhouette boundaries obtained from BRL-CAD data subsampled to about 100-150 data points; while in the second column we show the results of processing these boundary contours with the weak chain smoother. In Figure 6 through Figure 8 we give a progression of four characteristic polygons for the M60 tank, the M113 APC and the M35 truck, respectively. These sequences illustrate the uniformity and persistence in scale and angular sensitivity. In Figures 9 through 11 we show a complete progression of scale-space polygonalizations for the APC from fine to coarse resolution.

4.2 RESULTS FOR REAL IMAGE DATA

We have also tested the utility of the characteristic polygon filter in extracting edge boundaries detected in real thermal image data. Having obtained the characteristic polygon, if additional shape fidelity is required, one can define still another variational energy, this time a convex polygonal-spline energy, which indexes back into the original image at *knot points* along the perimeter of the characteristic polygon. Minimizing this cost over the vertices of the characteristic polygon by adapting an extension to the B-spline considered in [71] results in a polygon, not to be confused with a *control polygon* [63], which fine-tunes its final shape according to the image gradient. Thus, characteristic polygons can be considered as highly stabilizing pre-filters for *active contour models* [68], [73]. In this way the sides of the characteristic polygon can be slightly readjusted by indexing back into the gradient information in the original image. Although this operation requires iterated solutions to a full linear system, its cost is modest since the square dimension involved is given by the number of vertices of the characteristic polygon which is minimal by construction, typically from about one to two dozen.

In Figure 12(a) we show a close-up of an APC taken from a scene containing four APCs from CNVEO/Visionics' simulated FLIR imagery *trim2* database (image: cota0601). For edge quality comparison purposes we depict the Canny edges [66] for this image in Figure 14(a). The sequence of images given in Figures 12(b) and 12(c) give the intermediate images computed during the Canny edge detection process. Figure 12(b) shows the original image after smoothing with a Gaussian kernel and Figure 12(c) gives the image corresponding to the Euclidean norm of the image gradient of the smoothed image. Finally, the edge image in Figure 14(a) shows a close-up of the edges which result after optimizing over the norm of the gradient image and performing thresholding with hysteresis. In Figure 13(a) we show the weak continuity membrane image [65], [61] obtained with the parameters $\lambda = 16$ and $h_0 = 25$. The surface plot for this membrane image is given in Figure 13(b) and the corresponding edges are shown in Figure 14(b). Clearly the membrane images are superior to the Canny edges but at a significant cost, requiring about two and a half minutes to process this subimage. We next extracted a sequence of minimum bi-variance edges which we have developed to provide for fast edge extraction as discussed in [62]. In Figure 14(c) we give the characteristic polygon computed from the minimum bi-variance edges found. The characteristic polygon edges compare quite favorably with the membrane edges and Canny edges and were computed in about 5 seconds on a SUN IPC. This polygonalization was obtained using no post-processing for increased fidelity as discussed above.

5.0 CONCLUSIONS AND EXTENSIONS

We have described an innovative approach to multi-scale polygonalization of target silhouettes, as a means to construct economic target models for ATR. We have also demonstrated its utility and flexibility with examples from CAD and field imagery. Among future extensions planned, is the further development of a software suite that can automatically generate hierarchically catalogued views of the target silhouette having maximum economy with respect to range and view angle variations. Both CAD target models and field data will be accepted as input by the suite. The system will also provide for the modeling of internal boundaries using our multiresolution polygonalization methods.

6.0 REFERENCES

1. A. Rosenfeld and M. Thurston, "Edge and curve detection for digital scene analysis," *IEEE Trans. Comput.*, vol. C-20, pp. 562-569, May 1971.

2. A. Rosenfeld, M. Thurston and Y.H. Lee, "Edge and curve detection: Further experiments," *IEEE Trans. Comput.*, vol. C-21, pp. 677-715, July 1972.
3. L.S. Davis and A. Rosenfeld, "Detection of step edges in noisy one-dimensional data," *IEEE Trans. Comput.*, vol. C-24, pp. 1006-1010, Oct. 1975.
4. A. Rosenfeld and E. Johnston, "Angle detection on digital curves," *IEEE Trans. Comput.*, vol. C-22, pp. 875-878, Sept. 1973.
5. A. Rosenfeld and J.S. Weszka, "An improved method of angle detection on digital curves," *IEEE Trans. Comput.*, vol. C-24, pp. 940-941, Sept. 1975.
6. H. Freeman and L.S. Davis, "A corner-finding algorithm for chain-coded curves," *IEEE Trans. Comput.*, vol. C-26, pp. 297-303, Mar. 1977.
7. P.V. Sankar and C.V. Sharma, "A parallel procedure for the detection of dominant points on a digital curve," *Comput. Graphics Image Processing*, vol. 7, pp. 403-412, 1978.
8. R.L.T. Cederberg, "An iterative algorithm for angle detection on digital curves," in *Proc. 4th Int. Joint Conf. Pattern Recognition*, Kyoto Japan, Nov. 7-10, 1978, pp. 576-578.
9. B. Kruse and C.V.K. Rao, "A matched filtering technique for corner detection," in *Proc. 4th Int. Joint Conf. Pattern Recognition*, Kyoto Japan, Nov. 7-10, 1978, pp. 642-644.
10. M. Anderson and J.C. Bezdek, "Curvature and tangential deflection of discrete arcs: A theory based on the commutator of scatter matrix pairs and its application to vertex detection in planar shape data," *IEEE Trans. Pattern Anal. Machine Intell.*, vol. PAMI-6, pp. 27-40, Jan. 1984.
11. J.C. Bezdek and M. Anderson , "An application of the c-varieties clustering algorithms to polygonal curve fitting," *IEEE Trans. Syst., Man, Cybern.*,vol. SMC-15, pp. 637-641, Sept. 1985.
12. C.H. Teh and R. T. Chin, "On the detection of dominant points on digital curves," *IEEE Patt. Analysis and Machine Intell.* vol. II, no. 8, pp. 859-872, Aug. 1989.
13. R. Bellman, "On the approximation of curves by line segments using dynamic programming," *Commun. ACM*, vol. 4, p. 284, 1961.
14. B. Gluss, "A line segment curve-fitting algorithm related to optimal encoding of information", *Inform. Contr.*, vol. 5, pp. 261-267, 1962.
15. B. Gluss, "Further remarks on line segment curve-fitting using dynamic programming," *Commun. ACM*, vol. 5, pp. 441-443, Aug. 1962.
16. B. Gluss, " Least squares fitting of planes to surfaces using dynamic programming," *Commun. ACM*, vol. 6, pp. 172-175, Apr. 1963.
17. B. Gluss, "An alternative method for continuous line segment curve-fitting," *Inform. Contr.*, vol. 7, pp. 200-206, 1964.
18. C.L. Lawson, "Characteristic properties of the segmented rational minimax approximation problem," *Numer. Math.*, vol. 6, pp. 293-301, 1964.
19. R. Bellman, B. Gluss, and R. Roth, "On the identification of systems and the unscrambling of data: Some problems suggested by neurophysiology," *P. NAS US*, vol. 52, pp. 1239-1240, 1964.
20. G.M. Phillips, "Algorithms for piecewise straight approximations," *Comput. J.*, vol. 2 pp. 211-212, 1968.
21. U. Montanari, "A note on minimal length polygonal approximation to a digitized contour," *Commun. ACM*, vol.13, pp. 41-47, Jan. 1970.
22. M.G. Cox, "Curve fitting with piecewise polynomials," *J. Inst. Math. Appl.*, vol. 8, pp. 36-52, 1971.
23. U.E. Ramer, " An iterative procedure for the polygonal approximation of plane curves," *Computer Graphics Image Processing* , vol 1, pp. 244-256, 1972.
24. J. Slansky, R.L. Chazin, and B.J. Hansen, "Minimum perimeter polygons of digitized silhouettes," *IEE Trans. Comput.*, vol. C-21, pp. 260-268, Mar. 1972.
25. R.O. Duda and P.E. Hart, *Pattern Classification and Scene Analysis*, New York: Wiley, 1973, pp. 328-339.
26. I. Tomek, "Two algorithms for piecewise linear continuous approximations of functions of one variable," *IEE Trans. Comput.*, vol. C-23, pp. 445-448, Apr. 1974.
27. T. Pavlidis and S.L. Horowitz, "Segmentation of plane curves," *IEEE Trans. Comput.*, vol. C-23, pp. 860-870, Aug. 1974.
28. K. Reumann and A.P.M. Witkam, "Optimizing curve segmentation in computer graphics," in *International*

Computer Symposium, A. Gunther, B. Levrat, and H. Lipps, Eds. New York: Elsevier, 1974, pp. 467-472.
29. E. U. Ramer, "The transformation of photographic images into stroke arrays," *IEEE Trans. CAS*, vol. 22, no. 4, pp. 363-374, 1975.
30. K. Ichida and T. Kiyono, "Segmentation of planar curves," *Electron. Commun. Japan*, vol. 58-D, no. 11, pp. 689-696, 1975.
31. J. Vandewalle, "On the calculation of the piecewise linear approximation to a discrete function," *IEE Trans. Comput.*, vol. C-24, pp. 843-846, 1975. *Applied Optics* Vol.28 (1989).
32. T. Pavlidis, "A review of algorithms for shape analysis," *Computer Graphics Image Processing* , vol. 7, pp. 243-258, 1978.
33. T. Pavlidis, "Curve fitting as a pattern recognition problem," Proc. 6th Int. Conf. Pattern Recognition, 1982, vol. 2, pp. 853-857. *Computer Graphics Image Processing* , vol. 7, pp. 243-258, 1978.
34. C.M. Williams, "An efficient algorithm for the piecewise linear approximation of planar curves," *Computer Graphics Image Processing* , vol. 8, pp. 286-293, 1978.
35. W.A. Perkins, "A model-based system for industrial parts," *IEEE Trans. Comp.*, vol. 27, no. 2, pp. 126-143, 1978.
36. L.S. Davis,"Shape matching using relaxation techniques," *IEEE Trans. Pattern Anal. Mach. Intell.*, vol. PAMI-1, pp.60-72, 1979.
37. J. Slansky and V. Gonzalez, "Fast polygonal approximation of digitized curves," *Pattern Recognition*, vol. 12, pp.327-331, 1980.
38. T. Pavlidis, "Algorithms for shape analysis of contours and waveforms," *IEEE Trans. Pattern Anal. Mach. Intell.*, vol. PAMI-2, pp.301-312, 1980.
39. C.M. Williams, "Bounded straight-line approximation of digitized planar curves and lines," *Computer Graphics Image Processing* , vol. 16, pp. 370-381, 1981.
40. F. Badi'i and B. Peikari, "Functional approximation of planar curves via adaptive segmentation," *Int. J. Syst. Sci.*, vol. 13, no. 6, pp. 667-674, 1982.
41. T. Pavlidis, *Algorithms for Graphics and Image Processing.* New York: Computer Sci., 1982, pp. 281-297.
42. G. Dettori, "An on-line algorithm for polygonal approximation of plane curves," Proc. 6th Int. Conf. Pattern Recognition, 1982, vol. 2, pp. 840-842.
43. P.E. Danielsson, "Polygonal approximation of digital curves," *IBM Tech. Disclosure Bull.* vol. 24, no. 11B, pp. 6215-6217, 1982.
44. Li-De, "Consistent piecewise linear approximation," in *Proc 6th Int. Conf. Patter Recognition*, vol. 2, pp. 739-741, 1982.
45. Y. Kurozumi and W.A. Davis, "Polygonal approximation by the minimax method," *Computer Graphics Image Processing* , vol. 19, pp. 248-264, 1982.
46. K. Wall and P.E. Danielsson, "A new method for polygonal approximation of digitized curves," in *Proc. Third Scandinavian Conf. on Image Analysis*, pp. 60-66, Studentlitteratur, Lund, Sweden, 1983.
47. L.D. Wu, "A piecewise linear approximation based on a statistical model," *IEEE Trans. Pattern Anal. Machine Intell.*, vol. PAMI-6, pp. 41-45, Jan. 1984.
48. K. Wall and P.E. Danielsson, "A fast sequential method for polygonal approximation of digitized curves," *Computer Graphics Image Processing* , vol. 28, pp. 220-227, 1984.
49. J. Roberge, "A data reduction algorithm for planar curves," *Comput. Vision, Graphics, Image Processing*,vol. 29, pp. 168-195,1985.
50. J.T. Schwartz and M. Sharir, "Identification of Partially Obscured Objects In Two Dimensions By Matching of Noisy 'Characteristic Curves'", Tech. Report No. 165, Robotics Report No. 46, New York University, Dept. of Computer Science, June 1985.
51. J.G. Dunham, "Optimum uniform piecewise linear approximation of planar curves," *IEEE Trans. Pattern Anal. Machine Intell.*, vol. PAMI-8, pp. 67-75, Jan. 1986.
52. H. Imai, "Computational-geometric methods for polygonal approximations of a curve," *Comput. Graphics Image Processing*, vol. 36, pp. 31-34, 1986.
53. O. Baruch, "Segmentation of 2-D boundaries using the chain code," *SPIE Visual Commun. and Image Processing II*, vol. 845, pp. 159-166, 1987.

54. D.E. Dudgeon, J.G. Verly, and R.L. Delanoy, "An Experimental target recognition system for Laser Radar Imagery", *Proc. DARPA Image Understanding Workshop 1989*, pp. 479-506.
55. C.S.Fahn, J.F. Wang and J.Y. Lee, "An Adaptive reduction Procedure for the Piecewise Linear Approximation of Digitized Curves," *IEEE Trans. on Pattern Anal. Machine Intell.* vol. PAMI-11, pp. 967-973, Sep. 1989
56. S.W. Zucker, R.A. Hummel, and A. Rosenfeld, "An application of relaxation labeling to line and curve enhancement," *IEEE Trans. Comp.*, vol. 26, no. 4, pp. 394-403, 1977.
57. H. Asada and M. Brady, "The Curvature Primal Sketch," *IEEE Patt. Analysis and Machine Intell.* vol. PAMI-8, no. 1, pp. 2-14, 1986.
58. A. Blake, A. Zisserman, and A.V. Papoulias, "Weak continuity constraints generate uniform scale-space descriptions of plane curves," *Proc. ECAI, Brighton, England*, 1986.
59. B. Kimia, A. Tannenbaum and S. Zucker, "On the evolution of curves via a function of curvature," *preprint, McGill Research Center for Intelligent Machines*, 1990.
60. F. Attneave, "Some Informational Aspects of Visual Perception," *Psych. Rev.*, 61, 1954, pp. 183-193.
61. J.S. Baras, D.C. MacEnany and A. LaVigna, "Automatic Target Recognition Algorithms," Quarterly Progress Report on Contract DAAB07-90-C-F425, AIMS-TR-90-7, AIMS INC., December 1990.
62. J.S. Baras, D.C. MacEnany and A. LaVigna, "Automatic Target Recognition Algorithms," Quarterly Progress Report on Contract DAAB07-90-C-F425, AIMS-TR-90-7, AIMS INC., April 1991.
63. P.J. Besl, "Geometric Modeling and Computer Vision," *Proceedings of the IEEE*, Vol. 76, No.8, Aug. 1988.
64. G.L. Bilbro and W.E. Snyder *et al*, "Mean Field Annealing: A Formalism for constructing GNC-like algorithms," preprint *IEEE Trans. Neural Nets*, 1991
65. A. Blake and A. Zisserman, *Visual Reconstruction* MIT Press, 1987.
66. J. Canny, "A Computational Approach to Edge Detection", IEEE *Trans. Pat. Anal. and Mach. Intel.*, Vol. 8, No. 6, pp. 34-43, 1986.
67. P. Craven and G. Wahba, "Smoothing noisy data with spline functions: estimating the correct degree of smoothing by the method of cross-validation," *Numer. Math.*, Vol. 31, pp. 377-403, 1979.
68. M.A. Kass, A. Witkin and D. Terzopoulos, "Snakes: active contours models," *International Journal of Computer Vision*, 1:321-331, 1988.
69. Y. G. Leclerc, "Constructing Simple Stable Descriptions for Image Partitioning," *Int. Jour. of Comp. Vision*, 3(1), pp. 73-102. 1989
70. K. Melhorn, *Multidimensional Searching and Computational Geometry*, Springer-Verlag, 1984.
71. S. Menet, P. Saint-Marc and G. Medioni, "B-Snakes: implementation and application to stereo," *Proceedings Darpa Image Understanding Workshop*, pp. 720-726 Sep. 1990.
72. D. Mumford and J. Shah, "Optimal Approximations by Piecewise Smooth Functions and Associated Variational Problems," *Comm. on Pure and Appl. Math.* Vol. XLII,pp. 577-685, 1989.
73. R. Samadani, "Adaptive snakes: control of damping and material parameters," *SPIE Vol 1570 Geometric Methods in Computer Vision*, pp 202-213 1991.
74. J.M. Oyster and N.B. Lehrer, "Model-based Perceptual Grouping (MPG): A Cooperative-Competitive Approach to Shape Recognition in Neural Networks," in *Proceedings Darpa Image Understanding Workshop* II pp. 225-8 Sep. 1990.
75. C. Peterson and B. Söderberg, "A New Method for Mapping Optimaization Problems onto Neural Networks," *Int. J. Neural Systems* **1**, (1), pp.3-22 1989.
76. A. Witkin, "Scale-space filtering", in *From Pixels to Predicates* A. Pentland (Ed.) Ablex Publishing, pp. 5-19 1986.

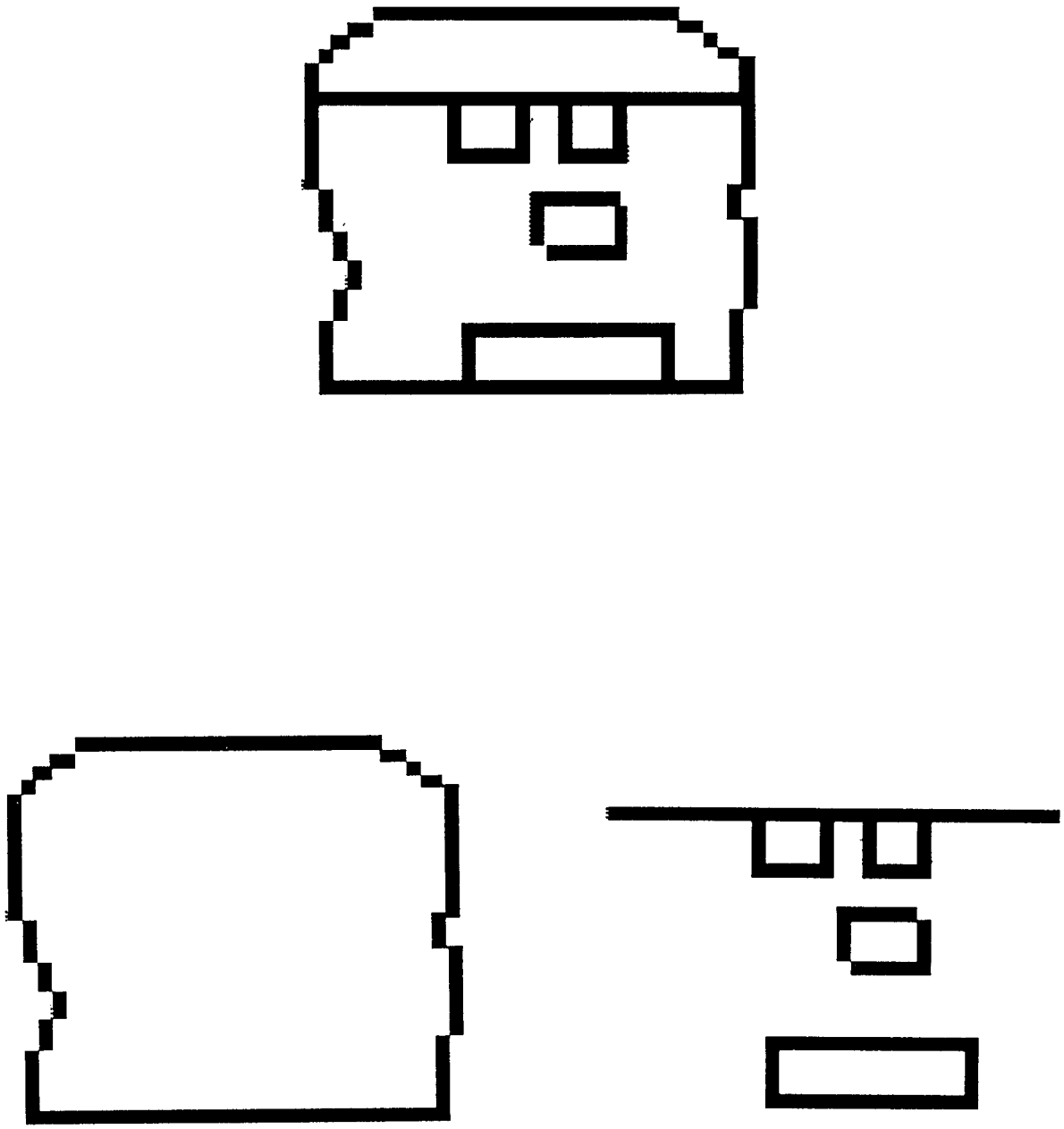

FIGURE 1.

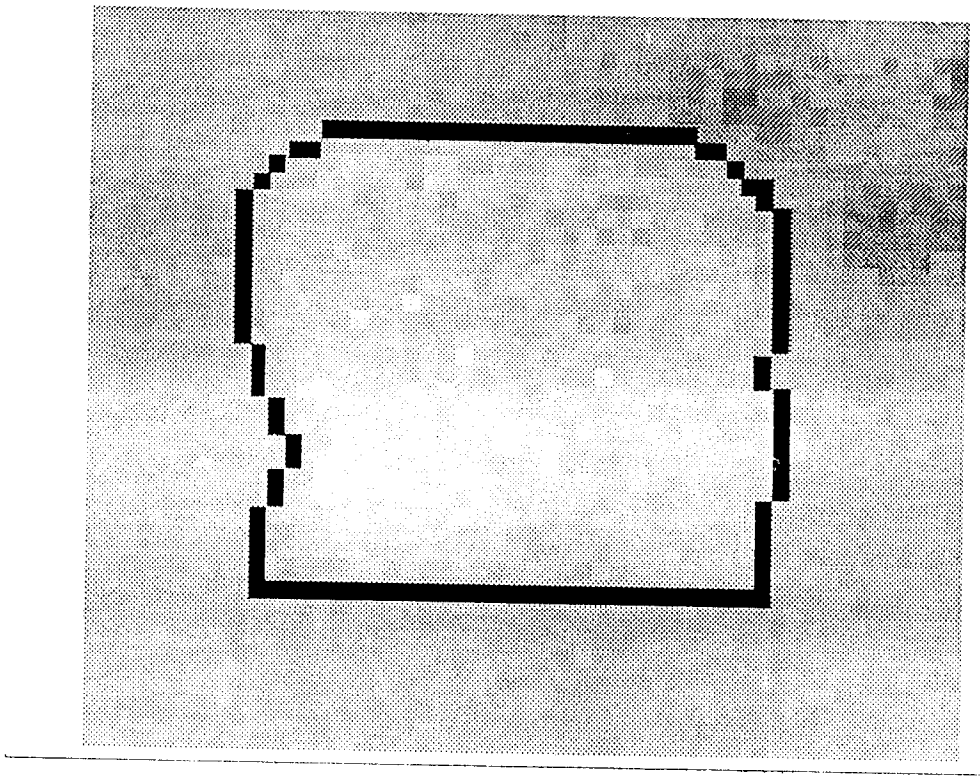

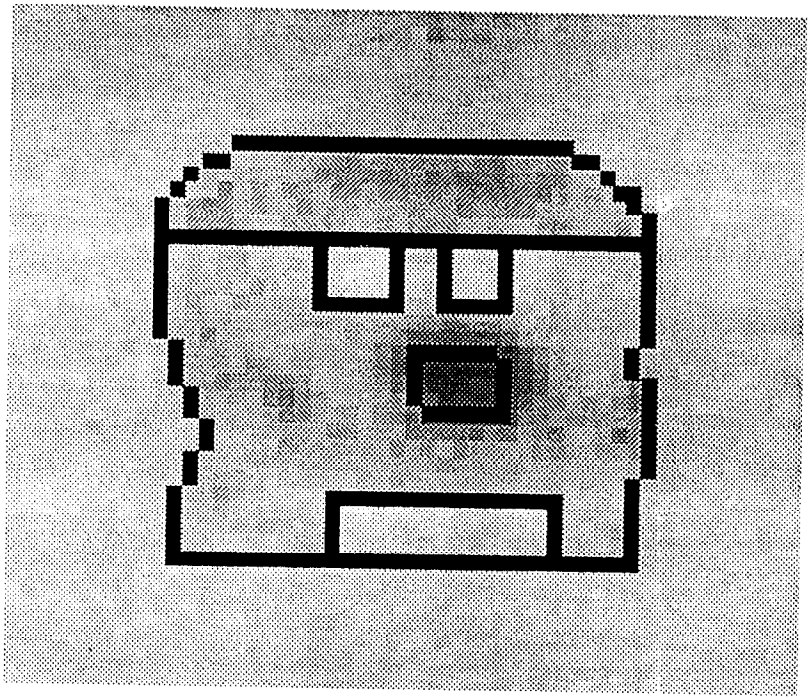

FIGURE 2

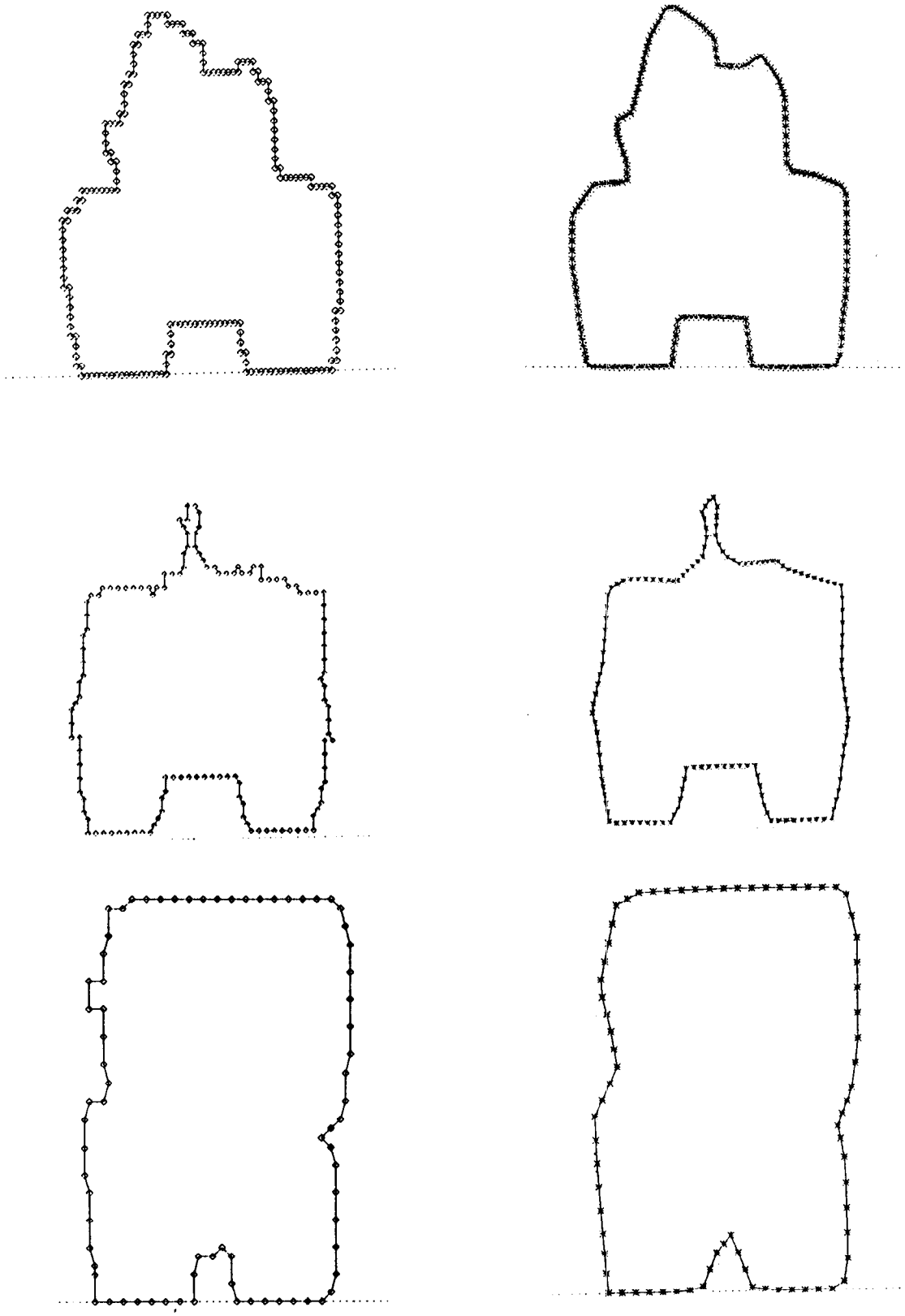

FIGURE 3

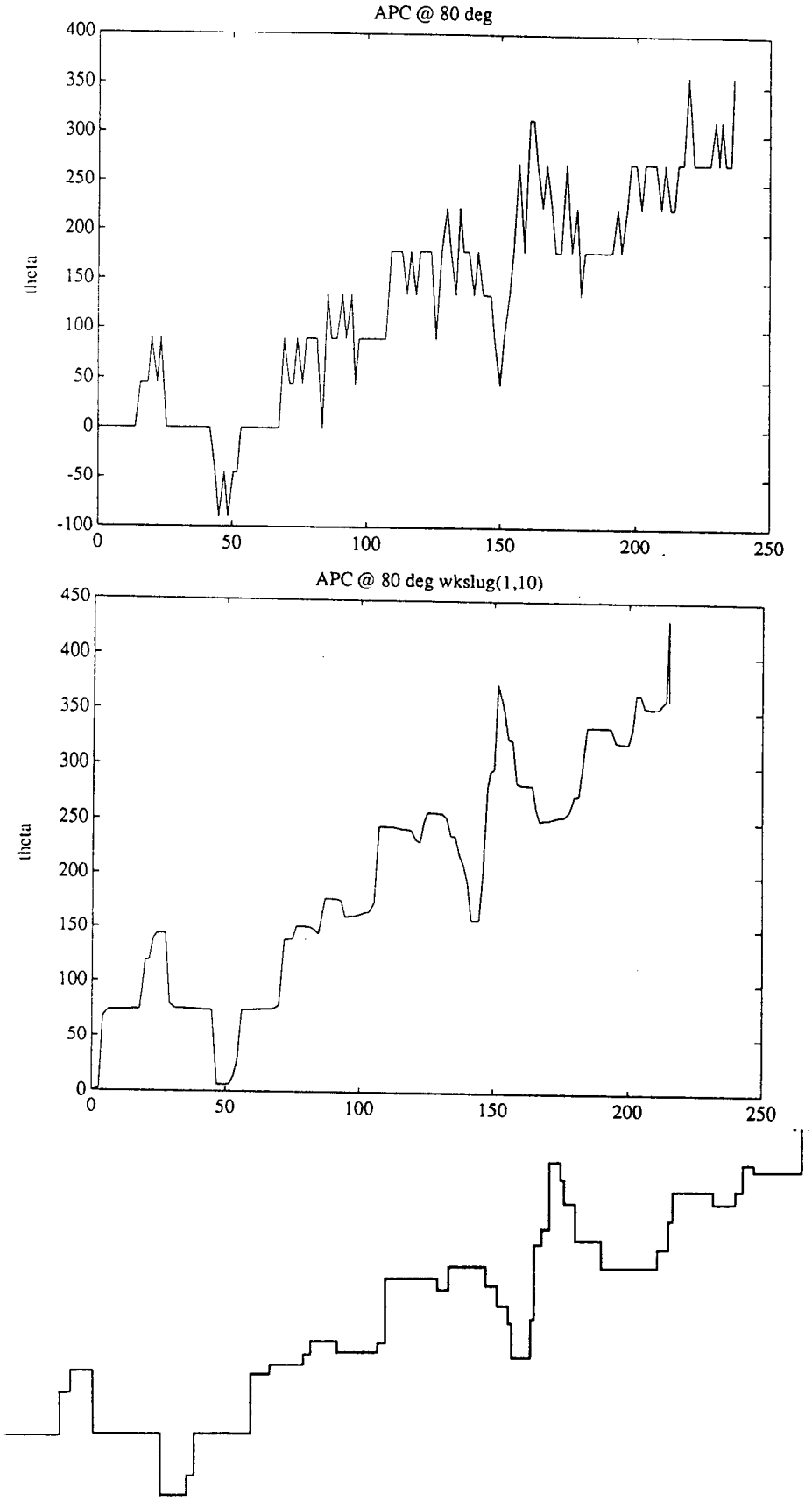
APC @ 80 deg
theta
400
350
300
250
200
150
100
50
0
-50
-100
0
50
100
150
200
250
APC @ 80 deg wkslug(1,10)
theta
450
400
350
300
250
200
150
100
50
0
0
50
100
150
200
250

FIGURE 4

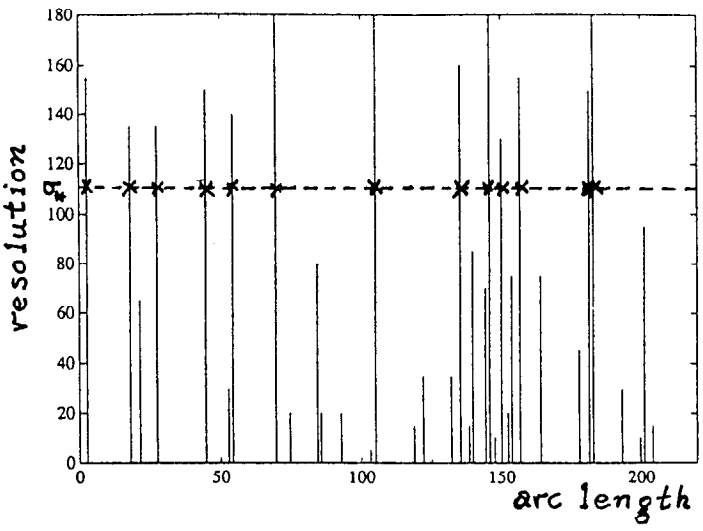
resolution q
arc length
0
20
40
60
80
100
120
140
160
180
0
50
100
150
200

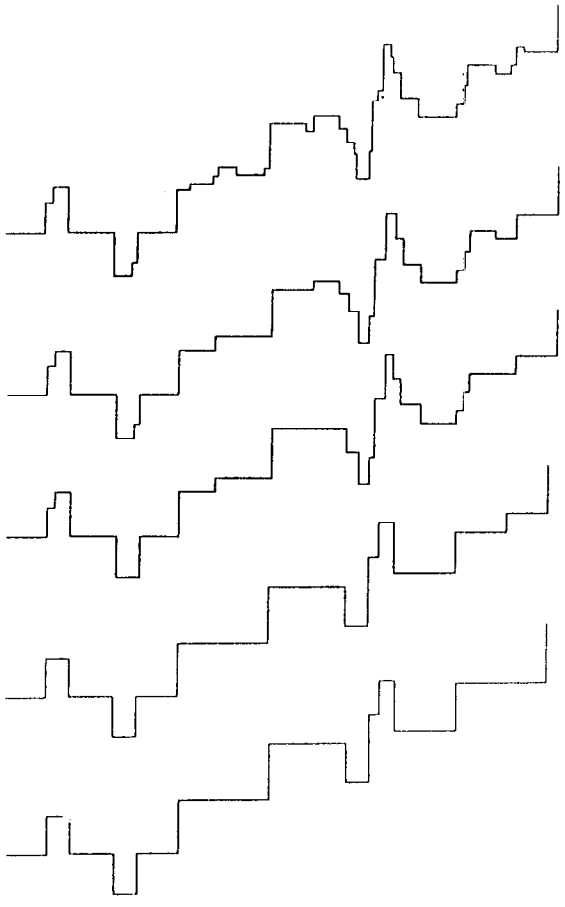

FIGURE 5

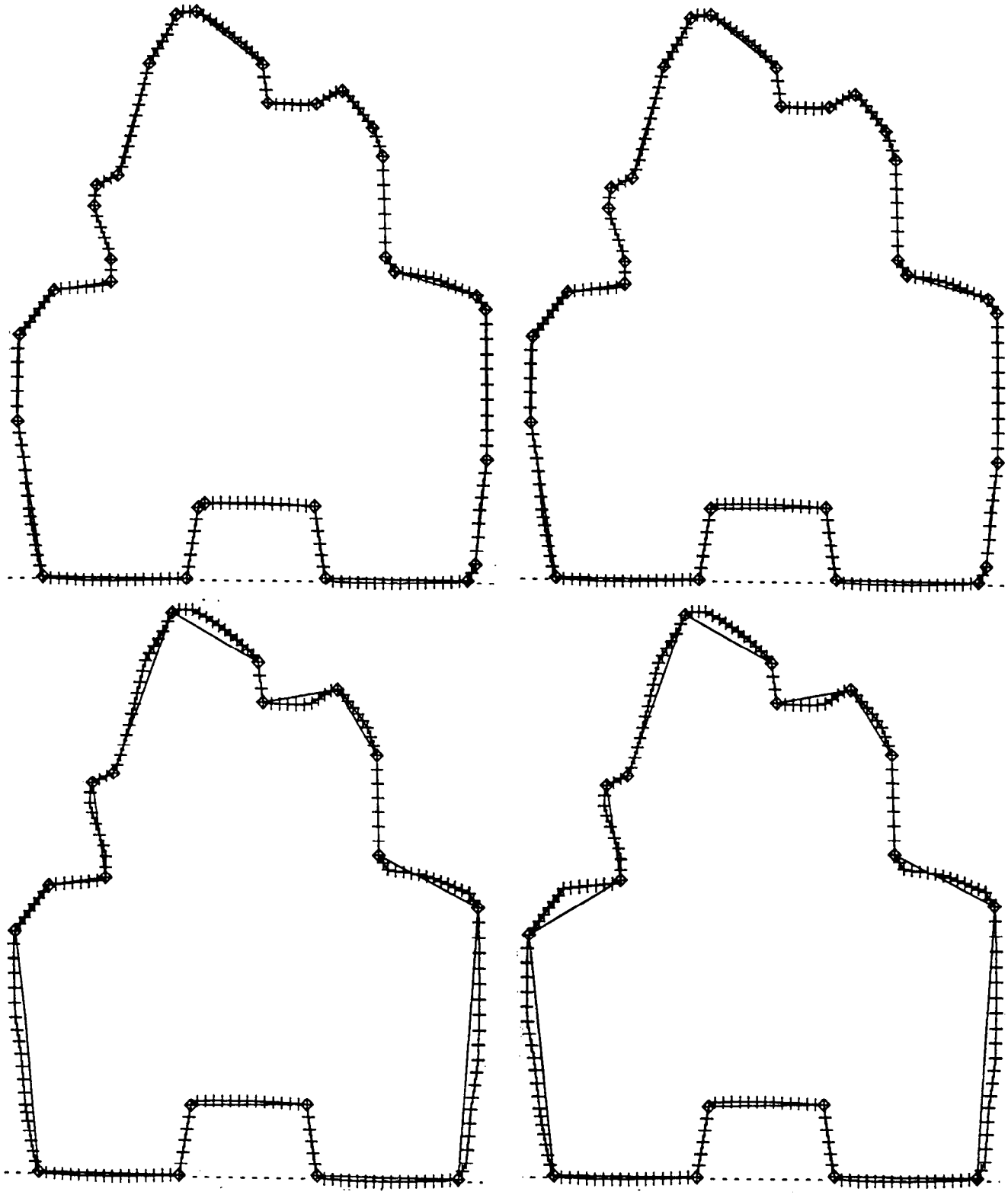

FIGURE 6

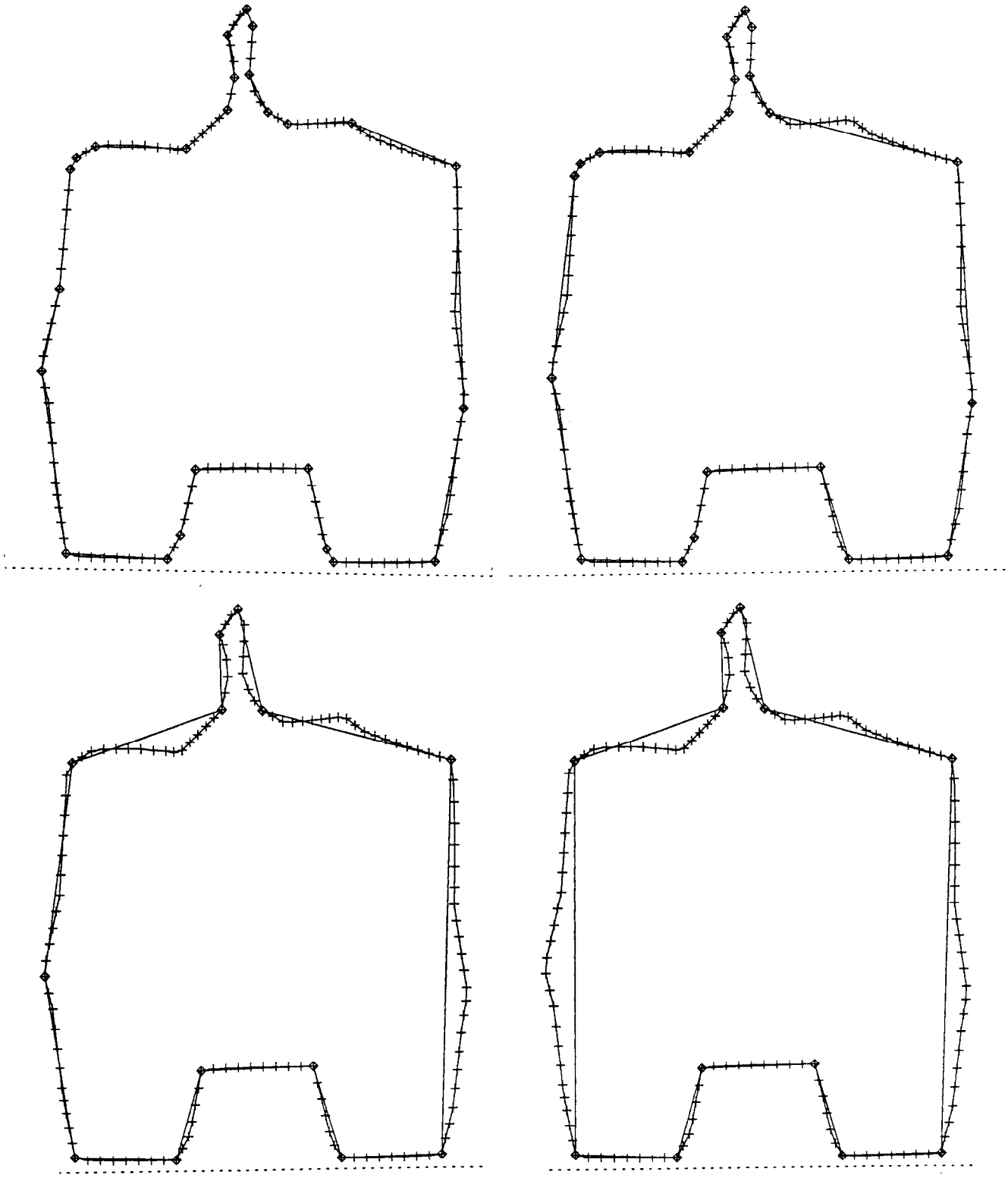

FIGURE 7

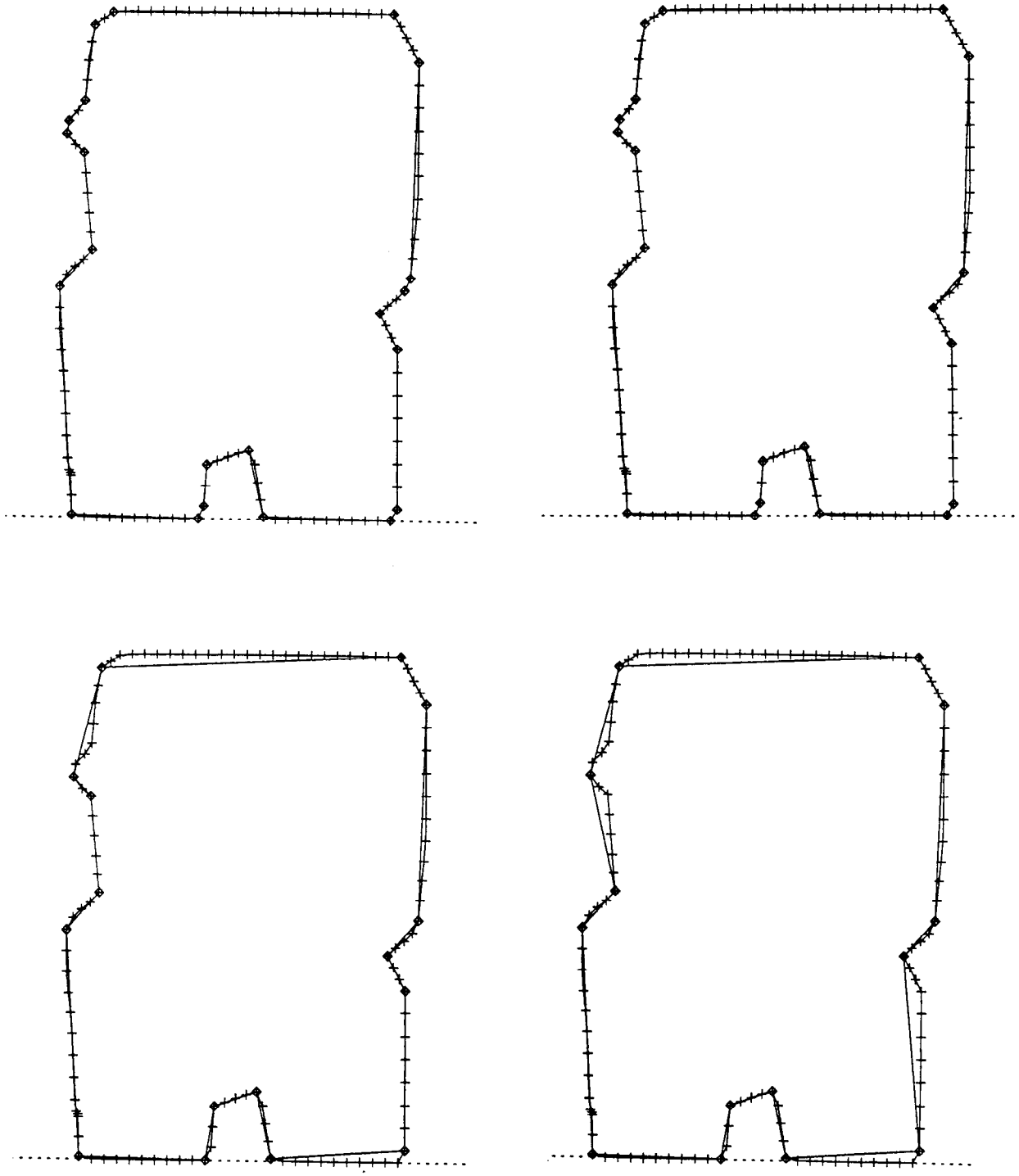

FIGURE 8

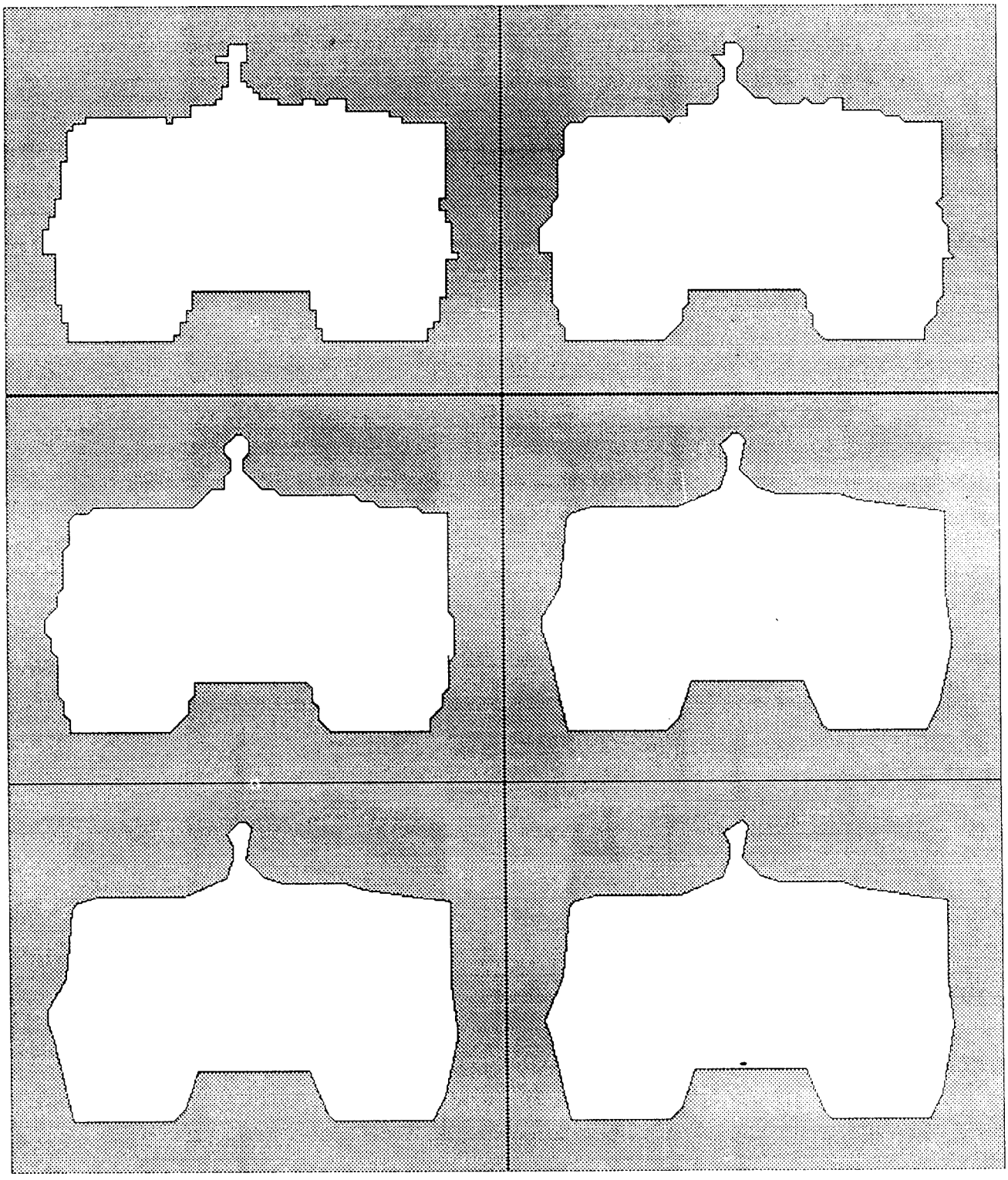

FIGURE 9

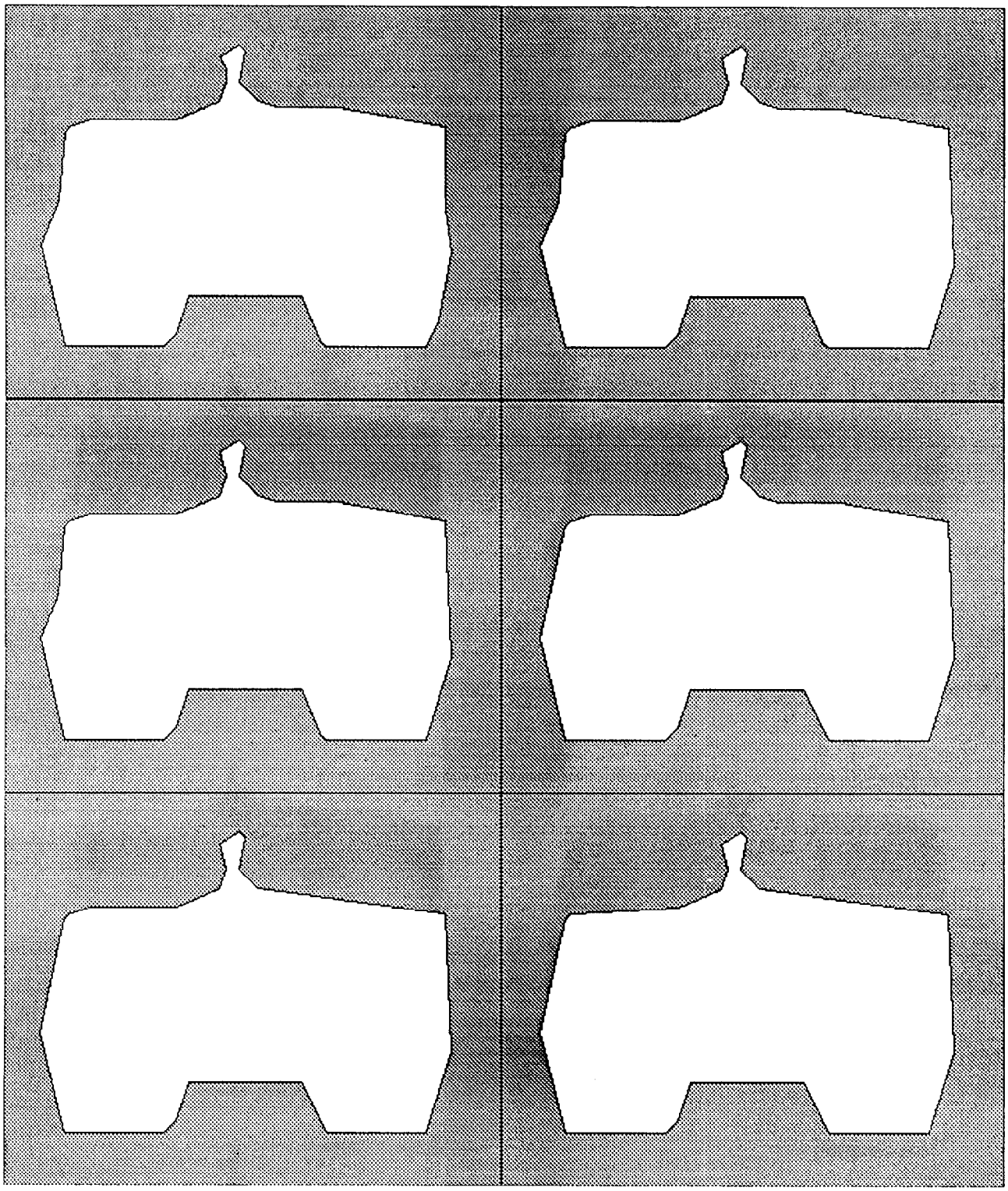

FIGURE 10

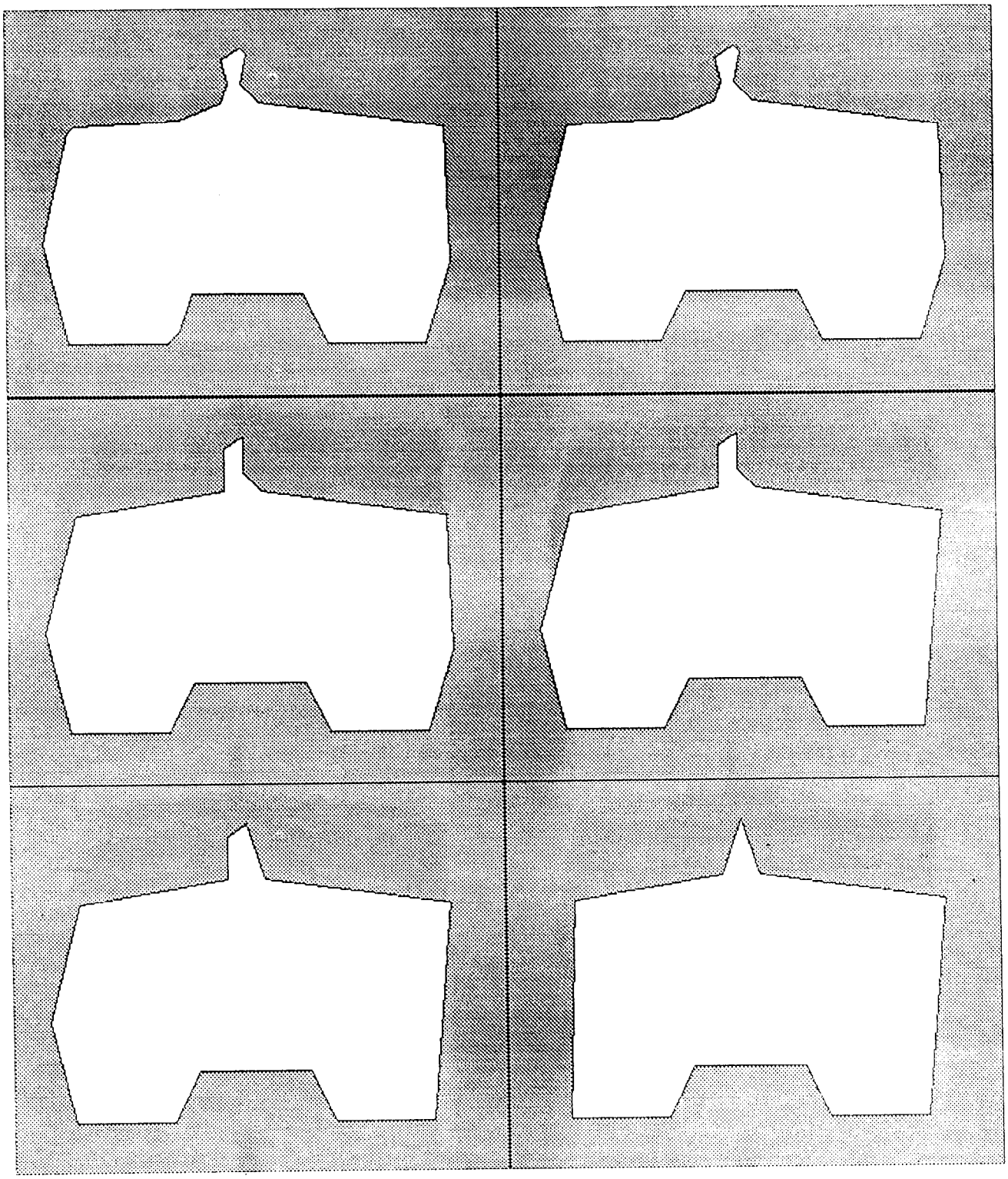

FIGURE 11

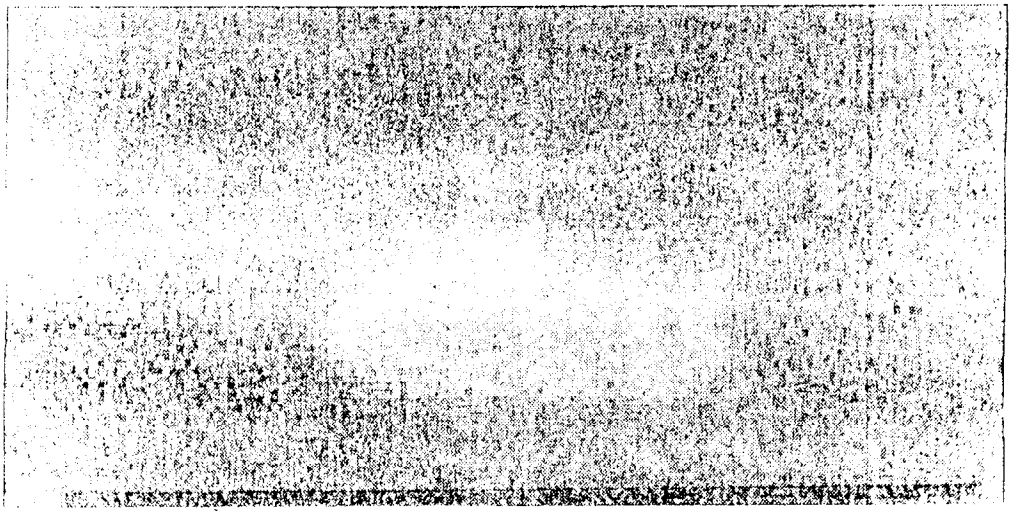

(a)

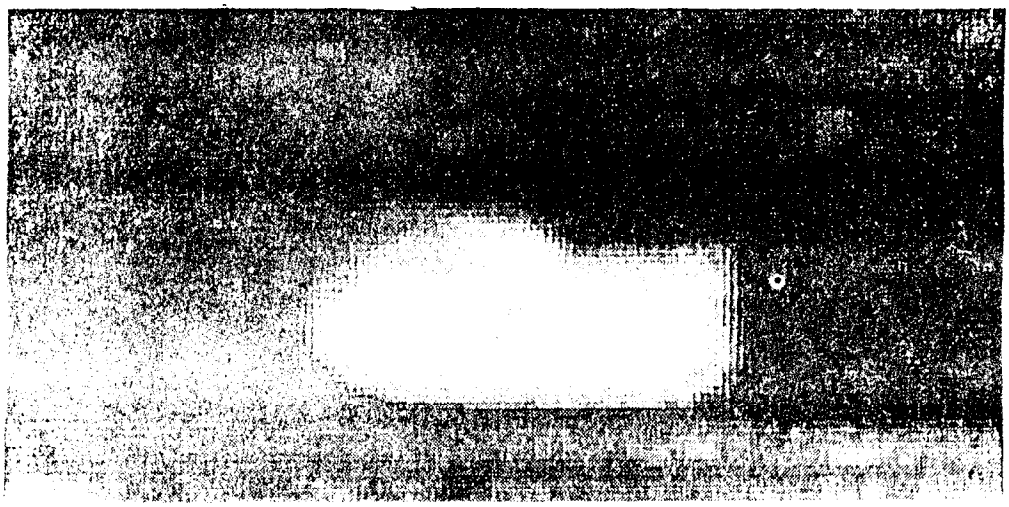

(b)

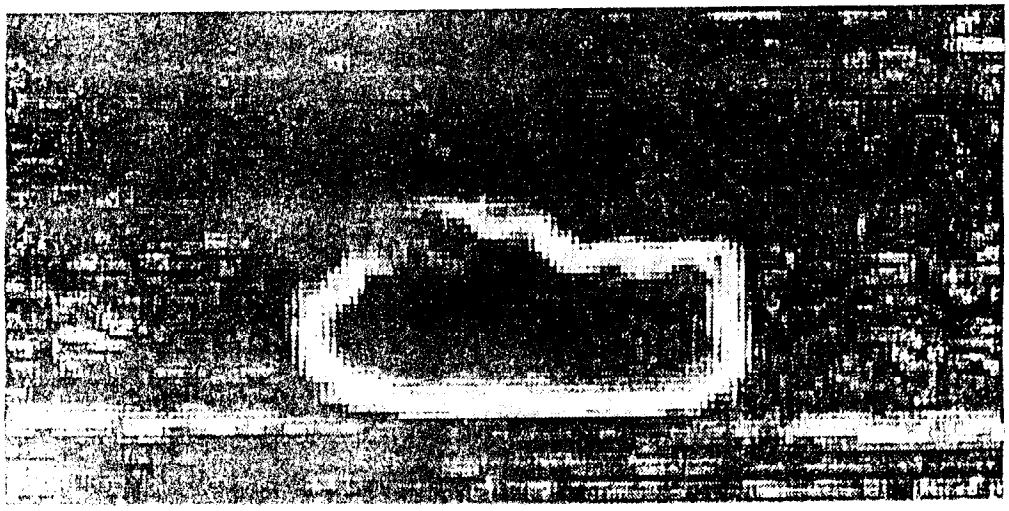

(c)

FIGURE 12

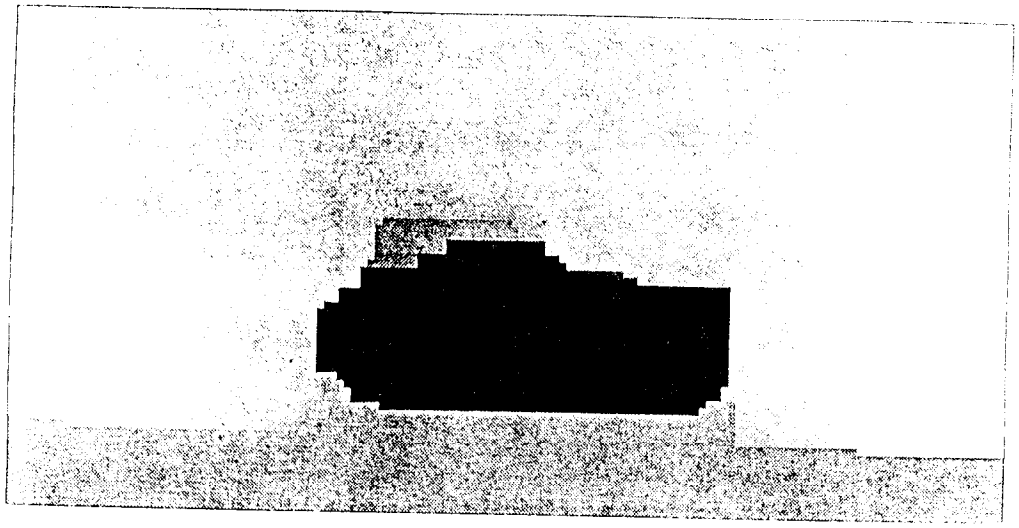

(b)

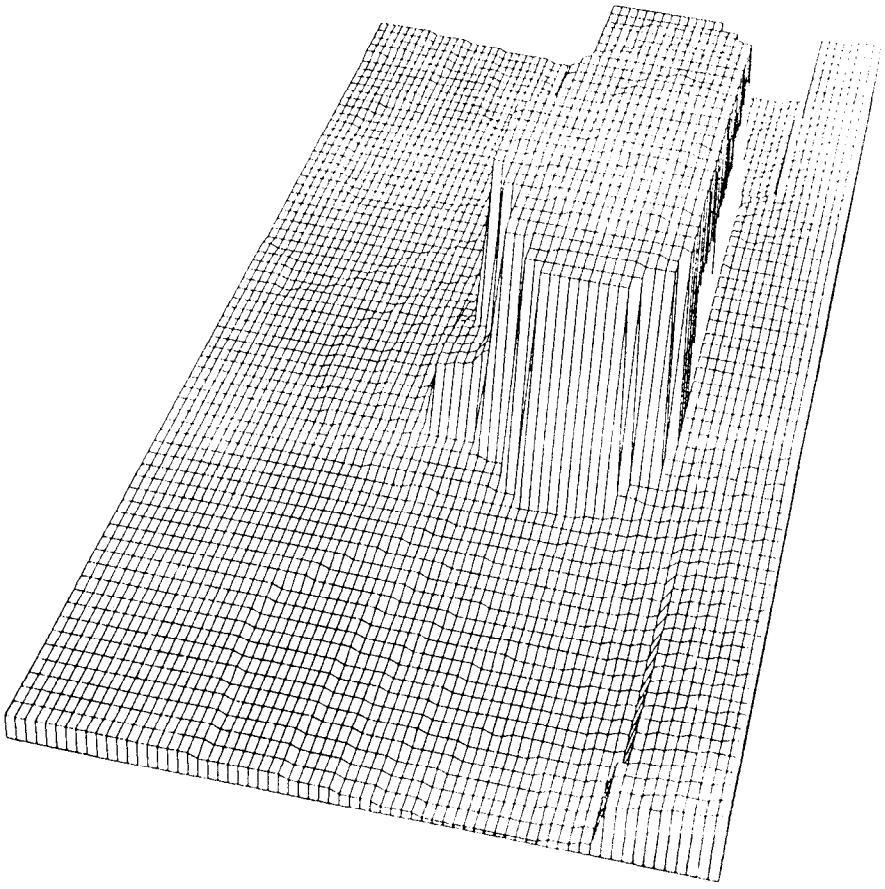

(c)

FIGURE 13

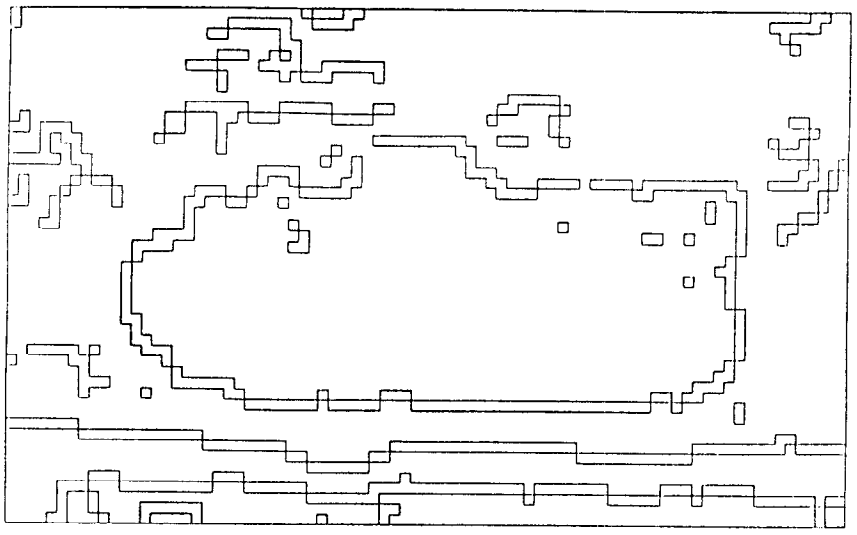

(a)

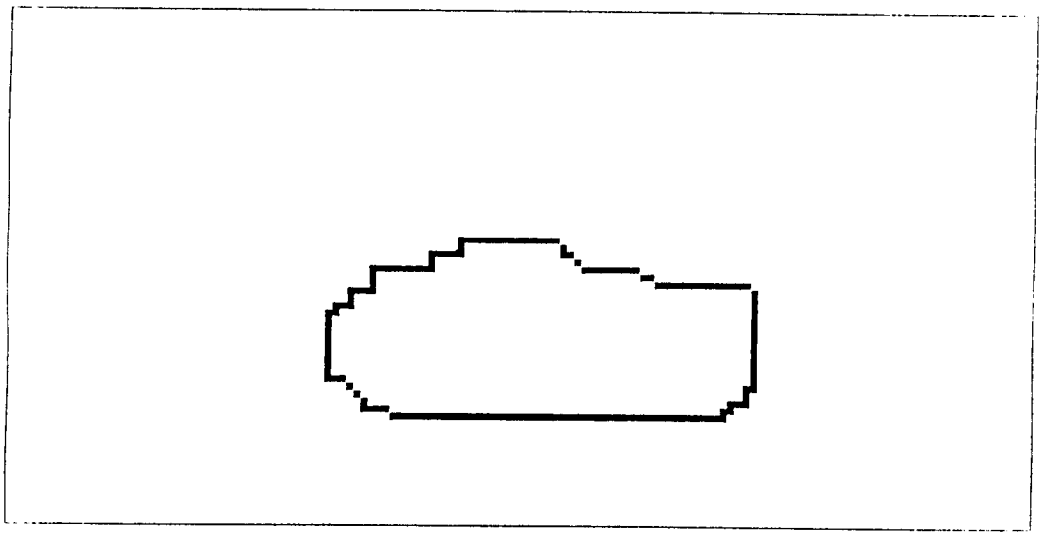

(b)

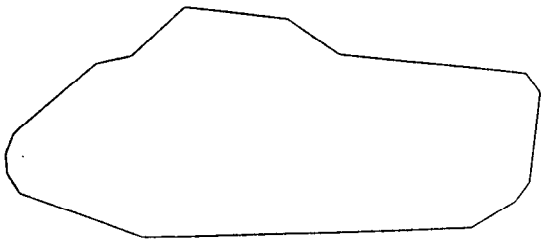

(c)

FIGURE 14